Potential Predictability of Malaria in Africa Using ECMWF Monthly and Seasonal Climate Forecasts

ADRIAN M. TOMPKINS

Abdus Salam International Centre for Theoretical Physics, Trieste, Italy

FRANCESCA DI GIUSEPPE

European Centre for Medium-Range Weather Forecasts, Reading, United Kingdom

(Manuscript received 11 June 2014, in final form 25 November 2014)

ABSTRACT

Idealized model experiments investigate the advance warning for malaria that may be presently possible using temperature and rainfall predictions from state-of-the-art operational monthly and seasonal weather-prediction systems. The climate forecasts drive a dynamical malaria model for all of Africa, and the predictions are evaluated using reanalysis data. The regions and months for which climate is responsible for significant interannual malaria transmission variability are first identified. In addition to epidemic-prone zones these also include hyperendemic regions subject to high variability during specific months of the year, often associated with the monsoon onset. In many of these areas, temperature anomalies are predictable from 1 to 2 months ahead, and reliable precipitation forecasts are available in eastern and southern Africa 1 month ahead. The inherent lag between the rainy seasons and malaria transmission results in potential predictability in malaria transmission 3–4 months in advance, extending the early warning available from environmental monitoring by 1–2 months, although the realizable forecast skill will be less than this because of an imperfect malaria model. A preliminary examination of the forecasts for the highlands of Uganda and Kenya shows that the system is able to predict the years during the last two decades in which documented highland outbreaks occurred, in particular the major event of 1998, but that the timing of outbreaks was often imprecise and inconsistent across lead times. In addition to country-level evaluation with district health data, issues that need addressing to integrate such a climate-based prediction system into health-decision processes are briefly discussed.

1. Introduction

Despite a reduction in range over the past century and a significant scale-up of control measures over the past decade, malaria remains a disease with a heavy health burden. The life cycles of the malaria parasite and its mosquito vector are affected by climate, principally temperature and rainfall (Craig et al. 1999). Thus, in addition to other factors such as land cover, human migration, interventions, and socioeconomic conditions that can alter the local disease prevalence significantly (Koram et al. 1995; Martens and Hall 2000), year-to-year fluctuations in climate can lead directly to variability in the intensity of malaria transmission. The malaria-parasite development time in both host and vector results in a temperature-dependent lag of approximately 1–2 months between the onset of suitably wet conditions for vector proliferation and symptomatic cases (e.g., Teklehaimanot et al. 2004; Bomblies et al. 2009). Thus, accurate real-time monitoring of temperature and rainfall conditions could provide useful information concerning malaria transmission in malaria early-warning systems (MEWS) 1–2 months in advance. Worrall et al. (2008) proclaim the cost effectiveness of well-planned interventions and emphasize the subsequent need for effective MEWS.

Mabaso and Ndlovu (2012) extensively reviewed articles that considered the relationship between climate and malaria in Africa and in particular those that attempted to employ the resulting information in MEWS through climate monitoring and/or forecasting. In particular, Rogers et al. (2002) highlighted the potential role of satellite monitoring of climate conditions in

Corresponding author address: Adrian Tompkins, ICTP, Earth System Physics, Strada Costiera 11, Trieste, TS 34151, Italy.
E-mail: tompkins@ictp.it

DOI: 10.1175/JAMC-D-14-0156.1

early-warning systems for malaria and called for improvements in disease-modeling capabilities to fulfill this potential. Hay et al. (2003a) also affirmed that rainfall monitoring could lead to improved planning potential. This was demonstrated in a case study for the Kenyan highlands, which also showed that the seasonal-forecast models at the time were inadequately skillful to extend the advance warning provided by rainfall observations (Hay et al. 2003b). The study also emphasized the fact that malaria case monitoring provided inadequate advance warning to implement mitigation actions, because outbreaks were only detectable once under way. Grover-Kopec et al. (2005) subsequently introduced a MEWS that was based on rainfall monitoring from satellite retrievals. The difference in advance warning, sometimes referred to as a forecast lead time, provided by case monitoring, climate monitoring, and climate forecasting was contrasted in Ceccato et al. (2007), emphasizing the additional potential gain in time for planners if skillful climate forecasts could be developed and successfully integrated into health-planning policy.

If the key environmental variables of temperature and rainfall could be accurately predicted using weather forecasts, warning of malaria outbreaks could potentially be provided earlier and on a regional or even continental scale. Until the most recent decade, the inaccuracy of dynamical forecasts of the weather in Africa precluded their effective use, but this situation has improved with the latest-generation systems (Kim et al. 2012). Jones et al. (2007) assessed past climate forecasts (hindcasts) conducted for the DEMETER project (Palmer et al. 2004; a list of many common acronyms is available at http://www.ametsoc.org/PubsAcronymList) to show that they could potentially have been used to predict the 1997 and 1998 highlands outbreaks in northwestern Tanzania. A landmark study by Thomson et al. (2006) also used the DEMETER hindcasts to drive a simple statistical model for malaria that was trained with country-averaged cases in Botswana and showed positive skill for this index in a cross-validation exercise up to 6 months in advance. In Africa, Botswana is a country with relatively high seasonal predictability because of strong teleconnections to El Ninõ–Southern Oscillation. The country was also chosen for the study because it has a long multidecadal health dataset for malaria, which is needed to derive the statistical model and is a rarity on the continent. Jones and Morse (2010) advanced this work by substituting the statistical malaria model with a more complex dynamical model, the Liverpool malaria model (LMM; Hoshen and Morse 2004), which was driven for a grid of points covering Botswana. Jones and Morse (2010) showed that the malaria forecasts demonstrated positive skill and economical value, in particular for low-malaria years. The lack of initial conditions for the malaria model meant that the LMM had to be "spun up" from idealized initial conditions, potentially reducing the system skill.

Jones and Morse (2012) repeated this study, using a more recent set of climate hindcasts that were conducted for the ENSEMBLES project (Weisheimer et al. 2009) and focusing this time on points in central and West Africa that are subject to high year-to-year variability, where climate is likely to play a more significant role in interannual transmission variations. The integrations were compared with malaria-model runs driven by the 40-yr European Centre for Medium-Range Weather Forecasts (ECMWF) reanalysis, and thus the validation was referred to as a "tier-2" validation (Morse et al. 2005), because it does not directly compare the malaria model with health or entomological data and thus maximizes the reported skill by not accounting for malaria-model error. Although forecast skill was absent in many regions, skill was positive and linked to temperature variability in the highlands of Cameroon and rainfall variability was key in parts of Niger and Nigeria in West Africa.

In this paper, the work of Jones and Morse (2010, 2012) is advanced in several ways. First, the previous studies all used stand-alone one-off hindcast datasets, including forecast systems that were not necessarily operational but rather were used for research purposes. Here, we construct an African malaria forecast system that is based on a fully operational, state-of-the-art weather and climate prediction system, combining monthly and seasonal forecasting systems together in an attempt to maximize climate prediction skill. Second, this system realistically initializes the dynamical malaria model rather than spinning up the model, again to maximize prediction skill. Third, we extend the analysis of Jones and Morse (2010, 2012) spatially by examining the skill across the continent of Africa in a single system. As in Jones and Morse (2012), the focus is on areas of high interannual variability in transmission, where climate plays a key role.

After using reanalysis-driven malaria integrations to define the regions of high interannual variability in malaria, the article reviews these malaria integrations to examine the maximum *potential* advance warning that could be achieved in malaria predictions using this prediction system in an operational context and then relates these results to the prediction skill in temperature and rainfall. The word "potential" is emphasized to stress that this is an idealized investigation whereby the skill of the climate-forecast-driven malaria model is evaluated using reanalysis-driven malaria integrations (a tier-2 evaluation). Thus, the skill of the malaria forecasts refers to the "maximum potential predictability," because it effectively neglects the effect of errors in the malaria model,

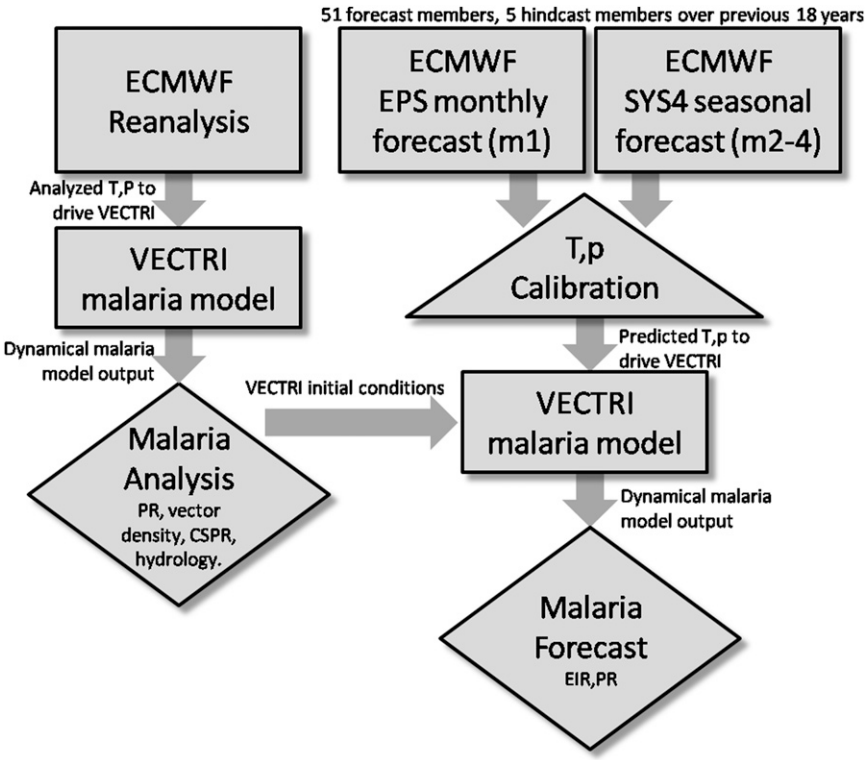

FIG. 1. Schematic of the forecast-system setup, with boxes representing models, triangles showing processes, and diamonds used for products. The operational NWP reanalysis of temperature and rainfall is used to drive the malaria model to provide a malaria analysis of epidemiological and entomological indicators, which are used as initial conditions for the forecast. The malaria forecast uses climate information from the high-resolution monthly EPS climate forecasts in the first month (m1, consisting of days 1–32), which is seamlessly combined with the seasonal-forecast system for m2–4. Both precipitation and temperature are rescaled, and temperature is calibrated before application to the malaria model, which then provides forecasts of PR and EIR.

which would reduce the actual skill below that reported in these investigations. This approach is adopted in this initial study because no continent-wide malaria-incidence dataset exists that can be used to evaluate malaria forecasts. One purpose of this study is thus to identify regions of the continent where the system demonstrates particular potential usefulness that can then be examined in future country-specific, focused studies that use the District Health Information System/Software (DHIS) and other health data.

2. Methods

a. *Overview of the malaria-prediction system and description of the weather-prediction model*

Our MEWS consists of two modeling components: a weather-forecasting system and a dynamical malaria model (Fig. 1). For the first 32 days of the weather forecast, the system uses temperature and precipitation that are provided by a high-spatial-resolution weather-prediction system. These forecasts extend the 15-day ensemble prediction system (EPS) out to 32 days once (recently increased to twice) per week, and at ECMWF is officially termed the extended-range forecast (Vitart et al. 2008). From day 33 onward, the forecasts of the lower-resolution and longer-range system-4 seasonal-forecasting system (Molteni et al. 2011) are used for the remainder of the 4-month forecast. To emphasize the difference in time scales of the two systems, they will be referred to respectively as the monthly and seasonal forecasts hereinafter. Both weather-forecast systems provide 51 individual forecasts starting from slightly different initial conditions so as to sample forecast uncertainty. Further details of the weather-forecasting systems that contribute to this seamless system are given in the appendix.

Temperature from both systems is adjusted using correction of the mean bias as a function of location, calendar month, and forecast lead time with respect to the analysis data and is subsequently statistically downscaled to 27-km resolution using a fixed lapse-rate correction to

account for the topography (Giorgi et al. 2003). This resolution is adequately fine to allow aggregation for comparison with district-level health data if required. The precipitation is also downscaled to this resolution using first-order conservative remapping [described in Jones (1999)]. One weakness of this first-generation system is that the precipitation forecasts are not currently bias corrected, implying that the mean simulated malaria transmission will be subject to systematic biases that can be caused by misplaced monsoon locations [e.g., see analysis of the earlier third release (''system 3'') of the ECMWF operational coupled seasonal-forecast system (SYS3) in Tompkins and Feudale (2010)] or mistimed rain onsets [Diro et al. (2012) examined SYS3 performance in the Horn of Africa]. Current research is investigating the relative performance of approaches that use matching of cumulative distribution functions (Piani et al. 2009; Hempel et al. 2013) vs approaches that are based on empirical orthogonal functions (Feudale and Tompkins 2011; Di Giuseppe et al. 2013a,b).

The above system produces daily precipitation and temperature forecasts. These forecasts are then used to drive the vectorborne disease community model of the International Centre for Theoretical Physics (referred to as VECTRI; Tompkins and Ermert 2013), a dynamical malaria model that is described briefly in the next section, to produce an ensemble of forecasts of a range of epidemiological and entomological measures.

b. *The malaria model*

A key component of the malaria-forecasting system is the VECTRI dynamical malaria model. It is fully described in the open-access paper by Tompkins and Ermert (2013); thus, only brief details are given here. The mathematical model solves a set of equations using a daily time step that describe the life cycles of the key vector *Anopheles gambiae* and the *Plasmodium falciparum* malaria parasite. Processes such as the gonotrophic cycle and the parasite and vector larvae-development rates are temperature sensitive, as are the mortality rates of the vector in the larval and adult stages. The combination of these temperature effects results in the model reproducing the observed nonlinear relationship between temperature and malaria, whereby malaria increases with temperature until a peak is reached between 25° and 30°C and decreases thereafter (e.g., Craig et al. 1999; Lunde et al. 2013).

Rainfall drives a simple representation for the fractional coverage of a grid cell by temporary water bodies, in a so-called pond parameterization. In the current version of the model, no spatial representation of permanent (year-round) open water bodies or wetlands is included. Although these certainly can be important local hotspots of year-round disease transmission (Carter et al. 2000; Bousema et al. 2012), it is recalled that they are unlikely to lead to year-to-year variations in malaria in response to climate, which is the focus of this study. In the majority of locations, the malaria season is strongly associated with the rainy season with a 1–2-month lag, indicating that the temporary ponds that are represented in the model are the key determinant of breeding-site availability.

The relationship between rainfall and malaria is strongly nonlinear: while rainfall drives the creation of temporary water bodies, the model also includes a representation of the flushing effect whereby intense rainfall increases the mortality of early-stage larvae (Paaijmans et al. 2007). Thus, in locations with low rainfall amounts, the intensity of malaria transmission increases with rainfall, but above a certain threshold the malaria transmission decreases with rainfall, as observed in Malawi and Botswana, for example (Thomson et al. 2005; Lowe et al. 2013). Note that the value for monthly rainfall at which transmission peaks will vary significantly both in time and space according to the subseasonal variability in rain events—rain falling in one or two extreme events separated by a dry break will promote far less transmission than the same rainfall amount falling evenly over a month. This effect is captured in the model, which operates on a daily time step, but this fact does imply that the model will be sensitive to the representation of the simulated daily rainfall distributions.

Similar to the LMM (Hoshen and Morse 2004), the VECTRI model uses a multicompartmental approach to resolve the key model processes. This is done because representing the delay between the onset of rainy conditions and the malaria-transmission season is important for forecasting purposes. One key feature of the VECTRI model is that it explicitly accounts for the human population density in the calculation of biting rates and host-to-vector and vector-to-host transmission probabilities for the parasite.

The key model-predicted variables are the parasite ratio PR and the entomological inoculation rate EIR (the number of infectious bites per person per time). For the skill assessment of the malaria forecasts, we use the *natural logarithm* of the EIR, however, rather than the EIR itself. The logarithm of EIR is relevant because it has been demonstrated to relate proportionally to morbidity in infants (Smith et al. 1998) and thus represents the nonlinear relationship between EIR and expected cases. In western and eastern Africa, a considerable number of isolated field studies have measured these indicators. Direct comparison with these field studies in

West Africa and the Malaria Atlas Project analysis for 2010 (Gething et al. 2011) shows that the VECTRI dynamical malaria model used in this forecast system can approximately reproduce the spatial distribution of EIR (see Tompkins and Ermert 2013) although the model simulation obviously cannot produce observations exactly because the model only accounts for climate, topography, and host population density and has no knowledge of interventions made to reduce transmission. Moreover, EIR measurements are often taken at single times and locations and are subject to large uncertainty that results from the sampling and calculation method.

Although VECTRI is a complex spatial model and was in fact the only fully dynamical model employed in two recent malaria-model intercomparison studies for future climate scenarios (Piontek et al. 2013; Caminade et al. 2014), several processes are neglected. There is currently a lack of treatment of host immunity; this lack is less important in areas where climate drives high year-to-year variability and host immunity is limited but remains a caveat on the results in intermediate transmission zones. Another simplification in the model is that it assumes bites received per person are randomly distributed, thus neglecting heterogeneities in the distribution of breeding sites relative to human habitations within a grid cell and also in host attractiveness to vectors (e.g., Knols et al. 1995), which changes the dynamic between EIR and PR (Smith et al. 2005). In summary, evaluation of the malaria model is ongoing, and, although preliminary evaluations of this new model are promising, the caveat that malaria-model inaccuracies will reduce actual malaria-forecast skill below the potential maximum should be kept in mind.

To assess forecast skill in predicting the metric of ln(EIR), we adopt the approach frequently used in NWP of comparing the forecast with the analysis (Simmons and Hollingsworth 2002). A direct comparison with clinical case numbers on a continental scale is not feasible because of the complexity of accounting for underreporting and misdiagnosis of fever cases, changes in identification (fever, microscopy, and rapid diagnostic test kits) over time, and differences in reporting systems among countries and the lack of access to such data in many countries (Checchi et al. 2006; Nankabirwa et al. 2009; Okiro and Snow 2010). Thus, here the aim is to present an analysis of the potential skill of the system on a pancontinental scale, with the emphasis on *potential* highlighting the neglect of malaria-model error that would result in lower effective skill. Areas with high potential skill can subsequently be examined on a country level using district-level case data. Results of such an undertaking conducted for the system in Uganda and Rwanda will be reported in a separate article.

c. *Malaria-model initial conditions*

One difference between this study and the work of Jones and Morse (2010, 2012) is that here the malaria model is initialized from realistic initial conditions. Any prediction of the future state of a system necessarily depends on the state conditions at the initial time. Therefore, to initialize the malaria-modeling component correctly the malaria-forecasting system requires an assessment of the important entomological and epidemiological variables such as vector adult and larvae density, circumsporozoite protein rate (CSPR), and PR in addition to the surface hydrological state, which gives the availability of breeding sites. Without this step, the malaria model would suffer from so-called spinup in the first weeks of the forecast as the model adjusts from idealized initial conditions, and valuable information concerning the climate conditions prior to the forecast start would be lost.

Borrowing the terminology widely used in the atmospheric numerical weather prediction (NWP) community, we refer to this assessment as the ''malaria analysis.'' It is important to stress that, in contrast to atmospheric analysis systems, the malaria analysis does not incorporate health or entomological observations. This is because direct observations of entomological variables are not generally available, given that they are collected in isolated research projects, and in any case are not available in near–real time, as is required for an operational framework.

We designed the analysis system using temperature and precipitation information from the operational ECMWF interim reanalysis system (ERA-Interim; Dee et al. 2011) to drive the malaria model and to provide malaria analyses of the relevant variables for each day from 1981 to the present. In common with all flux variables, precipitation is not directly available in the analysis and is thus derived from a short-range 24-h forecast starting from each 0000 UTC analysis cycle. The resulting analyses are used to provide initial conditions for each malaria forecast. Thus, if a forecast starts midway in a wetter-than-usual season, for example, the initial conditions will reflect this situation in terms of greater vector and larvae densities and more breeding sites available. The skill of the malaria forecasts is consequently not only affected by the skill of the climate forecasts but also in part derives from the knowledge of the climate anomalies that occurred prior to the forecast start that is contained in the malaria-analysis system. To our best knowledge, this is the first such dynamical forecasting system that attempts to

fully initialize the malaria-model component from an analysis system.

The choice of using reanalysis for this task was made with operational requirements in mind. First, it combines the available sparse, in situ measurements with the continuously changing remotely sensed information into a self-consistent assessment of the atmospheric state, thus maximizing continuity over time while ensuring continual spatial coverage and near-real-time operational delivery. For temperature, in situ measurements are sparse in many regions in Africa or are not available on the Global Telecommunications System in real time. Satellite retrievals of surface temperature are not available on a daily time scale or for long periods and can be subject to substantial errors over land (Li et al. 2013). The precipitation of the reanalysis is more reliant on the model's representation of moist physical processes. Nevertheless, many satellite-derived rainfall products are not available on a daily time scale or in near–real time. At the time that the system was constructed, the commonly available near-real-time, daily satellite products such as Famine Early Warning Systems (FEWS) Network rainfall estimates (Love 2002), the Climate Prediction Center morphing technique (CMORPH; Janowiak et al. 2005), and Tropical Rainfall Measuring Mission "3B42" (Kummerow et al. 1998) were not available for the entire 19-yr period to initialize the hindcast suite.[1] In any case, despite documented biases in the distribution of rainfall intensity and the rainfall mean, the reanalysis-derived rainfall is nevertheless capable of representing the intraseasonal variability over Africa, with Thiemig et al. (2012) demonstrating its competitiveness with some satellite-based products. Dutra et al. (2013) found that ERA-Interim rainfall could be successfully used in drought monitoring.

3. Results

a. *Identifying target zones*

Previous efforts to provide early warnings have pinpointed a selection of locations subject to sporadic epidemics or irregular short transmission seasons where adult immunity is lower (Doolan et al. 2009) and the intermittent transmission implies that health facilities may not be adequately prepared for significant outbreaks (Thomson and Connor 2001; Abeku et al. 2004; Cox and Abeku 2007). Jones and Morse (2012) also focused on areas with high year-to-year variability. This is important because in many locations climate variability will have a limited impact on year-to-year variability in malaria-transmission intensity. First, the relationship of the proportion of vector that survive sporogony as a function of temperature [e.g., see box 1 of Craig et al. (1999)] peaks in the range of 26°–33°C. The range of the peak depends on the vector in question and assumptions about mortality that are in the model (Lunde et al. 2013), but it is clear that in this range the malaria transmission will be relatively insensitive to temperature anomalies on the order of a degree, as compared with similar perturbations at the cooler or warmer limits of transmission, where malaria transmission probability changes more rapidly with temperature. Moreover, in highly endemic areas where the infant PR starts to saturate at high values, host dynamics are much more relevant for year-to-year variability, reducing sensitivity to interannual changes in climate (Hay et al. 2001). Thus, even if the underlying climate predictions prove to be accurate in highly endemic areas, climate-driven malaria forecasts are likely to be of limited usefulness. There is also the question as to how malaria forecasts would be of use for health planning in districts that are familiar with coping with regular seasonal transmission. The first step is therefore to locate areas and calendar months with high variability in malaria prevalence, using the daily malaria-analysis system.

The standard deviation of the PR for each calendar month provides insight to the modes of variability of malaria transmission, with Fig. 2 showing four example months. In each month examined, the standard deviation of PR shows three distinct modes. There is a mode at zero PR, which simply identifies malaria-free zones. The second mode identifies regions where the year-to-year standard deviation is nonzero but is less than ~10%, with the upper bound changing slightly from month to month. This mode is associated with endemic zones, where transmission regularly occurs in those months each year.

The last mode encompasses the remaining higher values of standard deviation exceeding 10%. The highest standard deviations belong to locations where transmission is very intermittent and does not occur every year but occurs instead in occasional epidemic outbreaks. Such events are termed a "true" or "classic" epidemic in the respective notations of Worrall et al. (2004) and Kiszewski and Teklehaimanot (2004). This mode also includes locations where transmission is regular each year but the transmission season is irregular in the particular month in question—for example,

[1] The second version of the FEWS Africa Rainfall Climatology product (ARC2) now covers the period 1983–present, although there are limited studies to evaluate the accuracy of this product, which does not use microwave information.

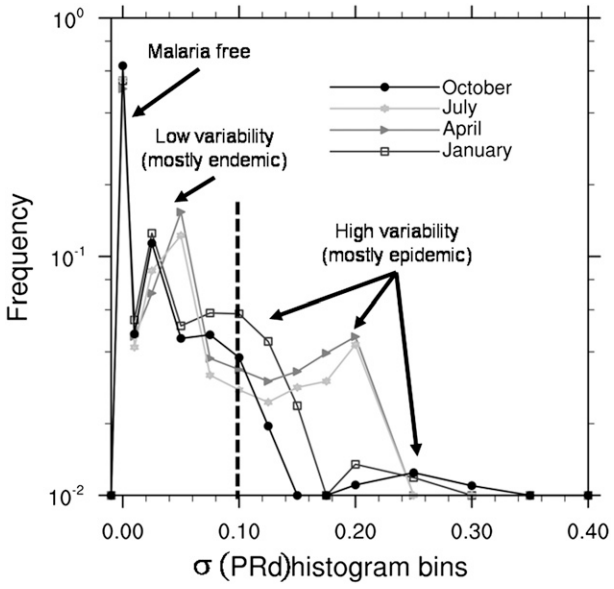

FIG. 2. Probability density function of the standard deviation of the PR for four representative months of the year. The vertical dashed line represents a standard deviation of 10% used as a threshold in the analysis to identify high-variability regions.

occurring later or earlier according to variability in the onset of monsoon rains. Thus, this mode also encompasses situations of ''unusual seasonal transmission'' (Worrall et al. 2004) and may include mesoendemic and hyperendemic zones.

On the basis of this analysis of the variability of rates of malaria prevalence, we subsequently identify all locations where the standard deviation of PR for a particular month exceeds 10% of the population to identify the epidemic model. To relate prevalence more closely to expected cases, an additional filter is applied to exclude months in which transmission intensity is minimal and no new cases are expected. This is accomplished by excluding months for which the EIR falls below 0.01 per month. The locations are then subdivided into two categories. The first category includes the hypo- and mesoendemic zones where immunity is likely to be lower and the malaria hazard affects the entire population. The second category concerns the hyperendemic regions, where children under age 5 are most at risk. Most holoendemic locations are excluded by the PR variability threshold since the interannual variation is low for all calendar months. This subdivision is made because malaria interventions and preparations are likely to differ in the two transmission environments. The separation of hypo/mesoendemic from hyperendemic regions is made using the common threshold of 0.5 for annual mean PR (Hay et al. 2004). This threshold can be applied to the whole population since the model neglects immunity, which increases rates of parasite clearance in adults relative to malaria-naive children but which also implies that the model will overestimate the area of the hyperendemic region relative to the lower transmission classes.

The resulting map in Fig. 3 identifies where and when a reliable malaria forecast would have a higher potential value to the decision maker. The map identifies epidemic regions such as the Sahel fringe, the East African highlands, and the southernmost transmission regions skirting through Botswana, southern Africa, and Mozambique. In each region the malaria model's representation of the vector and parasite life cycles results in a peak malaria transmission that is lagged with respect to the rainy season by 1–2 months. Using ''Afripop'' (Linard et al. 2012) population-density figures scaled to reproduce 2011 continent-total population estimates, 82.6 million people are estimated to live in epidemic regions. This number is lower than previous estimates (Snow et al. 1999; Worrall et al. 2004) as a proportion of the total population because of the VECTRI model's neglect of immunity, which in turn results in a positive bias in prevalence rates (Table 1). This population is divided almost equally between the Sahel region north of 10°N and the highland areas in the east and south of the continent.

It is in these zones that the indication of an outbreak by a reliable forecast could trigger a range of intervention strategies, depending on the status of the national malaria-control program in question (control, elimination, or postelimination surveillance). It is emphasized that this assessment is only for the theoretical climate-related variability of malaria and may not fully reflect the situation in reality. If control measures have led to local eradication, for example, then indication of heightened hazard due to climate anomalies may serve to tighten surveillance and response measures to imported cases in the region in question to prevent explosive growth of secondary cases (Moonen et al. 2010). Likewise, this assessment obviously neglects zones prone to epidemics as a result of nonclimatic factors such as forced population movements and breakdowns of health services as a result of conflict.

In addition to these epidemic zones, the map also reveals considerable areas with regular seasonal transmission but high variability in prevalence in certain months of the year, for example, in a band spanning the northern half of the Ivory Coast, Ghana, Togo, and Benin in West Africa during April and May. In these regions, malaria transmission variability is highest during the rain-season onset (also in April–May at these latitudes) and is associated with the interannual fluctuations of the monsoon cycle, which are highly variable

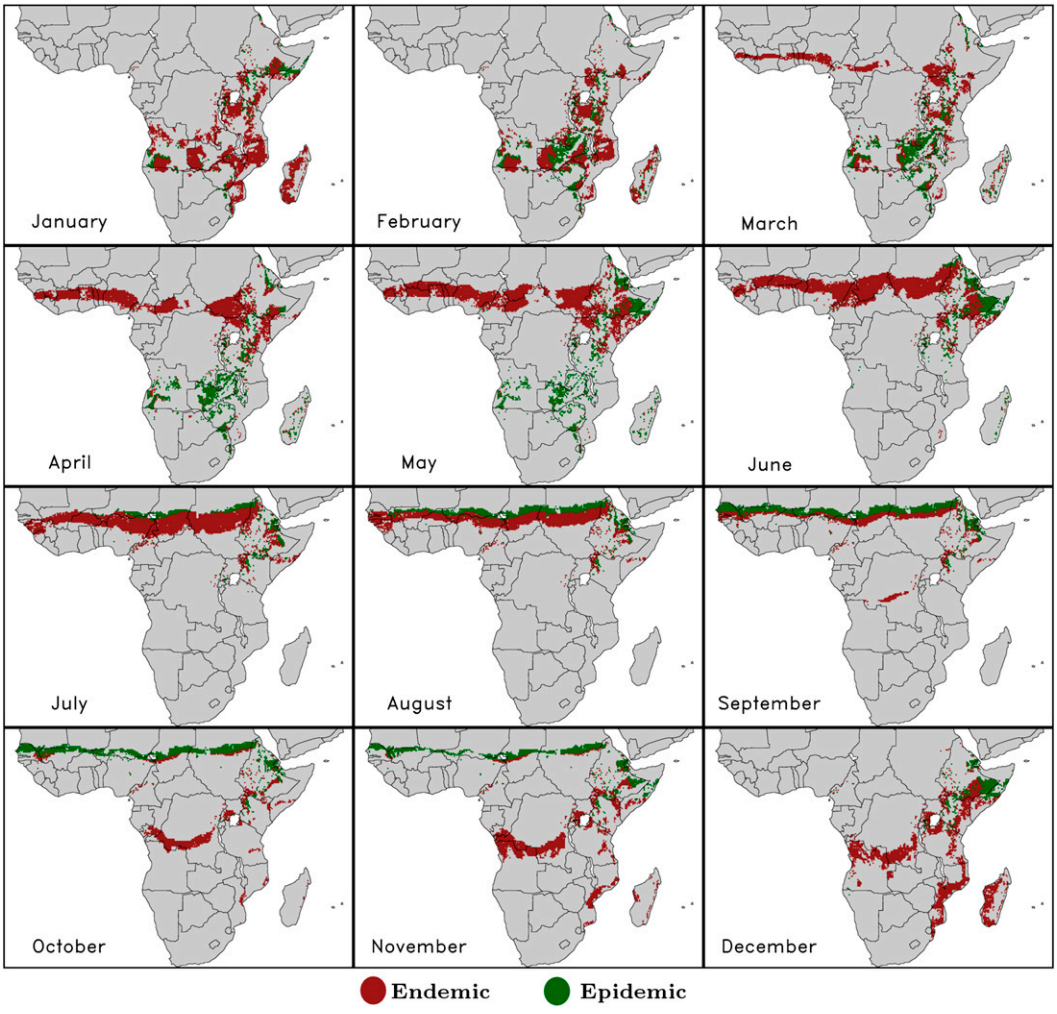

FIG. 3. Locations of high variability in parasite prevalence are shown for each calendar month of the year, subdivided into endemic (hyper- and holoendemic; red) and epidemic (hypo- and mesoendemic; green) transmission zones.

from year to year (Sultan et al. 2003). In these hyperendemic zones, health services are likely to be geared up to handle regular malaria transmission, unless funding shortages or breakdown of health structures preclude this. A skillful forecast could still be useful for ensuring timely mobilization of intervention actions involving insecticide-treated nets and/or indoor residual spraying (IRS) to maximize their impact (Worrall et al. 2008; Beier et al. 2008; Yukich et al. 2008). There could be significant cost savings associated with such planning-policy interventions when the considerable population of 400 million living in this area is considered (Table 1). Our subsequent analysis uses this analysis (Fig. 3) to exclude locations for each calendar month at which climate is deemed less relevant for interannual malaria-transmission variability.

b. *Potential predictability of malaria*

The skill of the forecast is examined for both the climate and malaria forecasts using the operational forecast-system output for 2012. We analyze the forecasts of 2012, and the 18 years of hindcasts, giving an

TABLE 1. Estimated 2011 population (millions) living in identified endemic regions subject to high-variability transmission 1 month or more per year, or epidemic regions. Regions are defined as north (lat $> 10°$), south (lat $< -10°$), central west ($|\text{lat}| < 10°$ and lon $< 20°$), and central east ($|\text{lat}| < 10°$ and lon $> 20°$).

	Africa	North	South	Central west	Central east
Epidemic	82.6	37.9	19.2	1.35	24.1
Endemic	404	137	48.0	118	101

evaluation period of 1994–2012. Although ideally one would evaluate an ensemble system using probabilistic skill scores, the small ensemble size of the hindcast (five members) prevents this, and thus the analysis is made for the skill of the ensemble mean anomaly correlation (Murphy and Epstein 1989). Temperature and calibrated precipitation are validated against the ERA-Interim reanalyses. We identify the locations at which skill in predicting malaria transmission is statistically significant 1–4 months in advance (referred to hereinafter as potential malaria-prediction skill) for each calendar month (Fig. 4). In addition to malaria, we show the skill in predicting anomalies of rainfall and temperature to identify which of these variables generate any identified malaria-prediction skill.

In examining first the shorter-range predictions 1 month in advance (Fig. 4, left column), it is encouragingly seen that there is model skill in malaria predictions in the target prediction zones throughout the calendar year. In some regions the predictability derives from correctly forecasting variations in temperature, but in southern Africa in a band stretching from Botswana through to Malawi and also across eastern Africa there are wide areas in which malaria-prediction skill is derived from both rainfall and temperature; for these areas, the analysis does not show which variable contributes most to the skillful malaria prediction. In these regions, rainfall predictability tends to be higher because of stronger teleconnections with the El Niño phenomenon (Ropelewski and Halpert 1987). Outside these regions, skill in precipitation prediction appears to be limited in the areas of interest for malaria forecasting, in broad agreement with studies using the predecessor of the seasonal forecast (SYS3) (Tompkins and Feudale 2010; Vellinga et al. 2012). This is confirmed in the analysis of the first-month rainfall skill in comparison with satellite retrievals conducted in the appendix.

In some locations the malaria forecasts are not significantly skillful, as marked by a limited number of black points where predictions of all variables fail, or by blue, purple, or red points, which indicate skill in climate prediction but not malaria prediction. In the northernmost Sahel belt spanning Senegal, Mali, and Niger in July and August, wide areas display skill in temperature only (red colors) while in some points rainfall is also correctly predicted (purple colors) but no potential malaria-prediction skill ensues. In this northernmost zone of the Sahel, rainfall variability and the northern extent of the monsoon limit malaria transmission (Thomson et al. 2004). Thus, where rainfall predictions are inaccurate, a frequent shortcoming in atmospheric models (Roehrig et al. 2013), malaria predictions will also fail. Where both rainfall and temperature are skillfully predicted, the failure to translate this into accurate malaria prediction could be related to the nonlinear relationship between transmission and rainfall in which intense rain events flush early-stage-larvae breeding sites (Paaijmans et al. 2007) and monsoon breaks lead to puddle desiccation (Gianotti et al. 2009). This nonlinearity is fully sampled by the high day-to-day variability of rainfall in the tropics; thus, significant skill in predicting seasonal rainfall anomalies may not be sufficient if subseasonal rainfall variability is poorly represented.

Analyzing the potential malaria-prediction skill for longer lead times of 2-4 months (Fig. 4, columns 2–4), it is seen that the climate-prediction system exhibits a sharp drop in skill at predicting rainfall and temperature 2 months in advance relative to 1 month. Despite this, there are wide areas for which the pilot MEWS still has significant skill for malaria prediction in months 2 and 3 and, in smaller regions, even 4 months ahead. This is due to the inherent lags between the rainfall anomalies and the resulting malaria-transmission season, such that the skill in predicting malaria transmission in the second and third months derives from the climate information contained in the forecast initial conditions and the first-month forecast of climate. This highlights the crucial role that the malaria-analysis system has in correctly initializing the malaria-modeling system. In areas where rainfall and temperatures are predictable beyond 1 month, such as in eastern Africa, the malaria-prediction advanced warning is extended beyond the 3-month range. The analysis thus indicates that by driving the malaria model with dynamical climate forecasts, useful information regarding the future transmission season in epidemic regions and seasonally variable endemic regions can potentially be delivered at least 1 and, in limited regions, 2–3 months earlier than would otherwise be the case using climate observations, which themselves provide more advance warning than the direct monitoring of symptomatic malaria cases (Thomson et al. 2006).

c. Uganda and Kenya highlands

To illustrate the potential value of the system in a real epidemic scenario, we examine the past performance over the East African highlands. The outpatient data of highland regions of southwestern Uganda and western Kenya have received considerable attention in the literature. In fact, in their comprehensive review of articles examining the relationship between climate and malaria, Mabaso and Ndlovu (2012) found

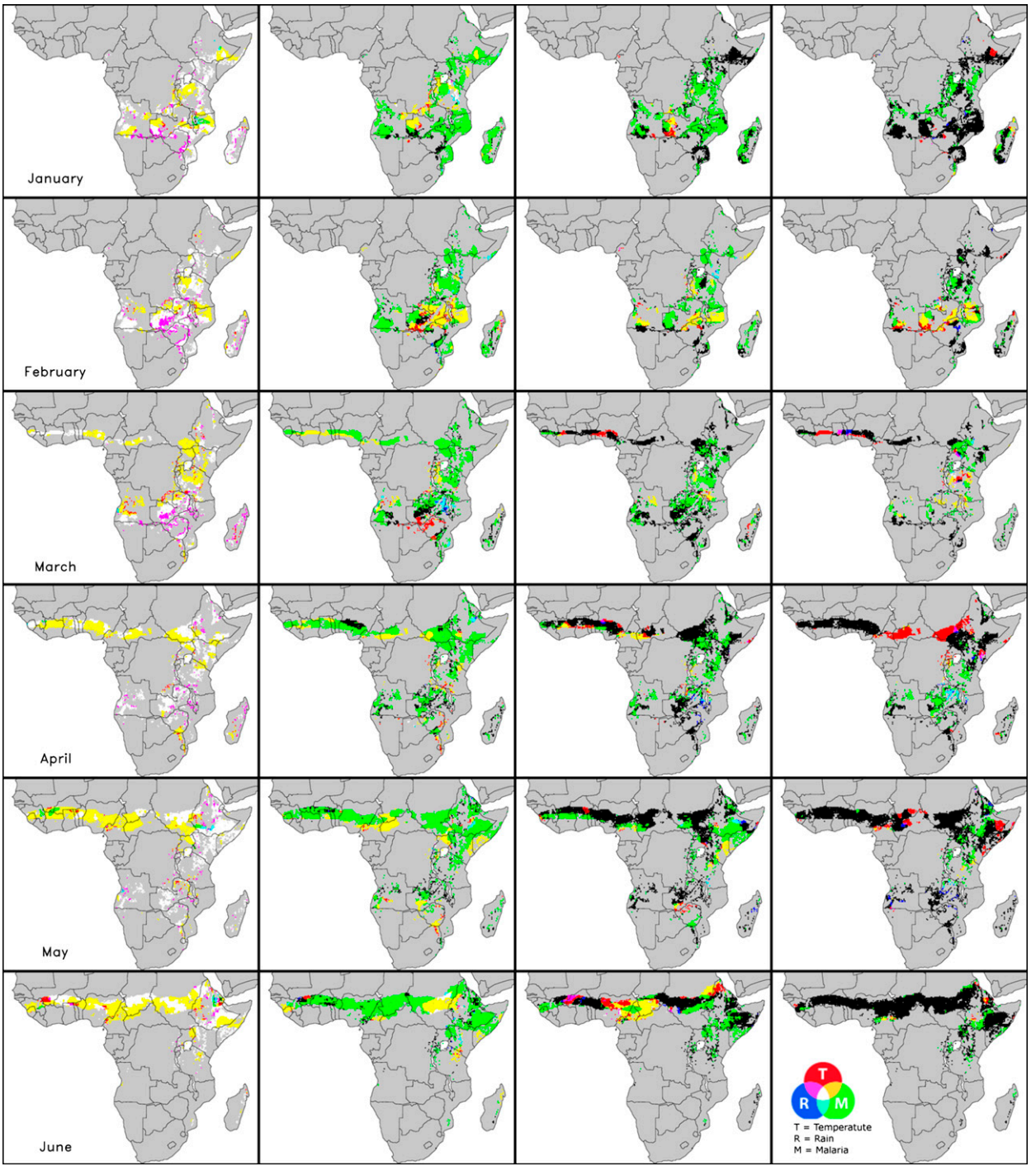

FIG. 4. Composite plot of temperature (red), precipitation (blue), and malaria [ln(EIR); green] forecast anomaly-correlation coefficients that are statistically skillful at the 95% confidence level for issuing warnings for (left) 1, (left center) 2, (right center) 3, or (right) 4 months in advance (lead time) for each calendar month of the year. White points mark cells with skill in all three variables; black points mark cells without any skill. See legend for color definitions of intersecting categories.

that this region was the most studied. Table 2 gives a qualitative and brief summary of the key malaria-transmission anomalies in highlands of western Kenya and/or Uganda between 1995 and 2010. The summary of the data is that a significant epidemic occurred in early 1998 across the region in the highlands that has been extensively described and has been linked to the major El Niño event of 1997–98

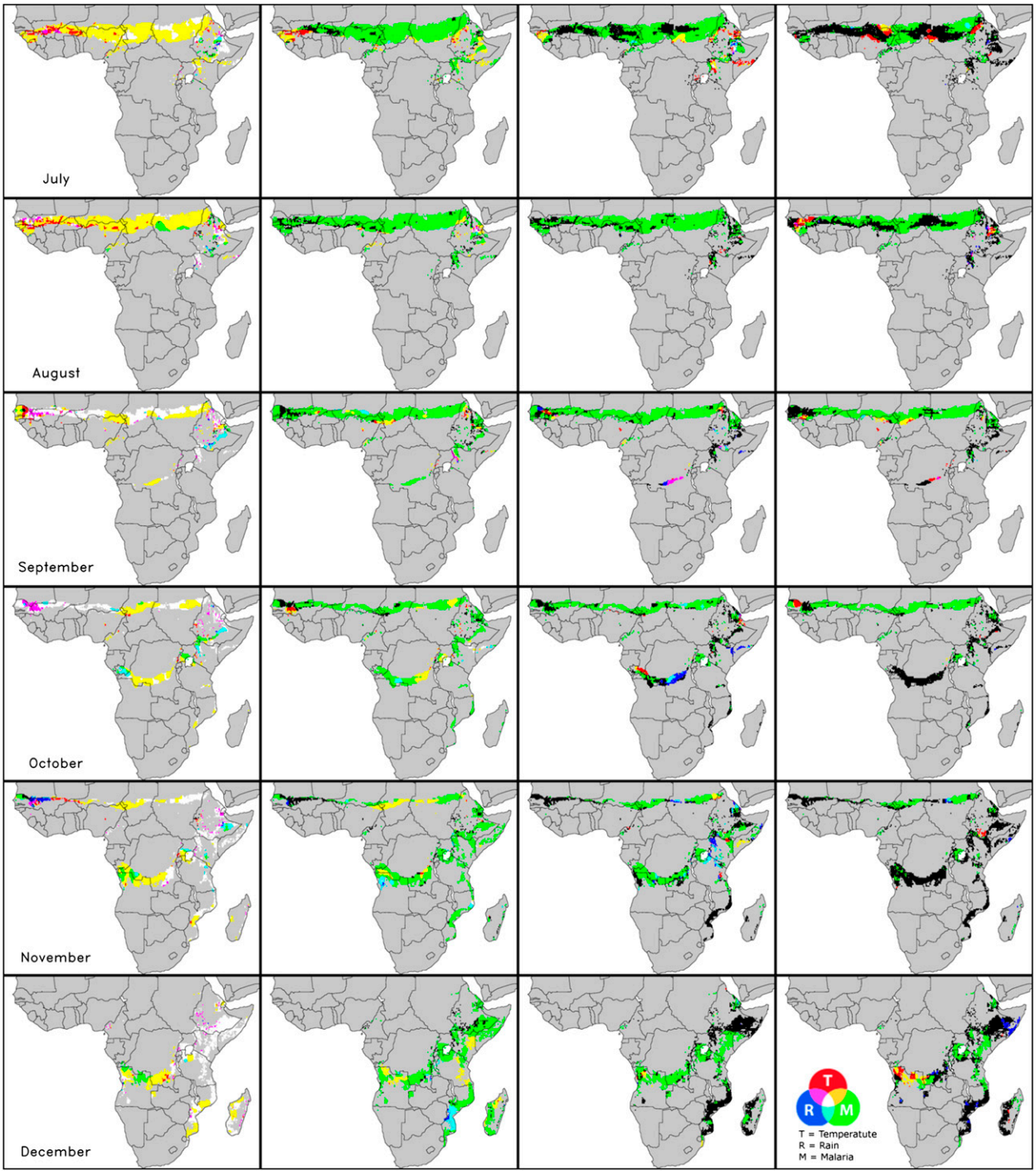

FIG. 4. (*Continued*)

(Lindblade et al. 1999; Githeko and Ndegwa 2001; Alonso et al. 2011). The other articles cited described evidence of more minor anomalies in transmission during 1994–95, 2002, 2005, 2006, and 2009–10, with the term ''minor'' employed in a broad sense to variously imply short-lived, less intense, or geographically restricted outbreaks.

To make an initial qualitative comparison with the forecasting system, the average normalized value of the ensemble-mean predicted ln(EIR) is analyzed for all

TABLE 2. Summary of selected literature that discusses epidemic conditions in the highlands of Uganda, west Kenya, or Tanzania.

Year	Reference	Summary
1994	Alonso et al. (2011)	Higher than usual transmission indicated in Kenyan highlands
1998	Lindblade et al. (1999)	Epidemic starts in Feb in Ugandan highlands; authors associate outbreak with rainfall anomalies
1998	Githeko and Ndegwa (2001)	Epidemic in Kenya from Feb 1998, but high incidence also reported in Jun–Jul 1997
1998	Jones et al. (2007)	Epidemic in Tanzania highlands from Feb to Jun 1998, and high incidence also reported in summer of 1997
2002	Hay et al. (2003a)	Epidemic identified in Nandi and Kericho in Jun–Jul, with conditions returning to normal in August; normal transmission occurred in the Kisii and Gucha districts
2005	Cox et al. (2007)	Examines DHIS data from 2002 to 2006 for Kabale and identifies outbreaks in 2005 (timing not described) and 2006 (centered on Jun) but questions the authenticity of the latter outbreak by using confirmed data from a sentinel site
2010	Ototo et al. (2011)	Report vector densities over the period from Sep 2009 to Apr 2010, reporting peak vector densities in Jan–Feb 2010; no long-term dataset is available to determine whether conditions were anomalous
2010	Yeka et al. (2012)	Describes general transmission in Uganda; smear-positivity rates for children under 5 show relative peaks in Kanungu District (Kihihi) for Oct–Dec 2009 and May–Jul 2010 (their Fig. 4); no anomalies in selected high-transmission zones

points at heights exceeding 1500 m (the results were insensitive to this altitude threshold) in a region spanning 28°–36°E and 2°S–2°N, with each month considered separately to remove the annual cycle of malaria transmission. A running mean of 5 months is also applied.[2] The forecast time series is then classified into three alert levels, where an amber alert signifies an upper-tercile event and a red alert signifies a value that exceeds the 90th percentile. We emphasize that these tercile thresholds are chosen because they are commonly employed in meteorological forecasting circumstances but may have little relevance to the decision-making process of, for example, a national malaria-control program. A full cost–loss analysis of suitable interventions is required to determine suitable thresholds for action, and thus the alert levels should be strictly viewed as indicative and illustrative.

The resulting time series (Fig. 5) is encouraging because it clearly shows that the major outbreak starting in February of 1998 is predicted 4 months ahead and is by far the most significant event predicted during the period 1995–2012, in qualitative agreement with the observations. In addition, all forecast lead times indicate lesser events occurring in 1995, 2002, 2005, 2006, and 2009–10. On closer examination, however, it is clear that the timing of the predicted events is often inaccurate. The main 1998 event is predicted to reach the highest alert level in February–March 1998, but the event appears to last too long, with the alert level remaining throughout 1998. Likewise, the event in 2005 appears to be well predicted 4 months in advance but is weaker and too early in the shorter-lead-time forecasts. High levels of transmission in 2006 appear to continue into 2007, which does not appear to be confirmed in the literature. Moreover, in general, there is a tendency for epidemic alerts to occur earlier in time in the shorter-range forecasts (e.g., 2002, 2005, 2006–07, and 2010). This could be related to a drift in the bias characteristics of the forecast precipitation, which is presently not bias corrected in the system. In summary, although the system shows promise at predicting during which years epidemic conditions are likely to occur, there remains much to be done to improve the representation of subseasonal fluctuations in transmission, while again emphasizing the highly qualitative nature of this initial comparison, which amalgamates all highland areas in Uganda and western Kenya into a simple single index.

4. Discussion: Integrating climate information into health planning

We have introduced a pilot dynamical forecasting system for malaria that is the first available on a continental scale that uses the highest-resolution monthly and seasonal ensemble prediction systems to drive a dynamical malaria model that is realistically initialized. These results have demonstrated the potential for skillful malaria predictions up to 4 months in advance over wide areas that were identified to have highly variable transmission for specific months of the year. This shows for the first time that climate forecasts may usefully extend the early warning available from environmental monitoring on a continental scale and reaffirms the potential importance of accurate climate information in Africa (Thomson et al. 2011). It is important to emphasize that this study is a first step and is

[2] This simple smoothing using a centered filter window could not be applied in real-time forecasting scenarios because the future months are not available.

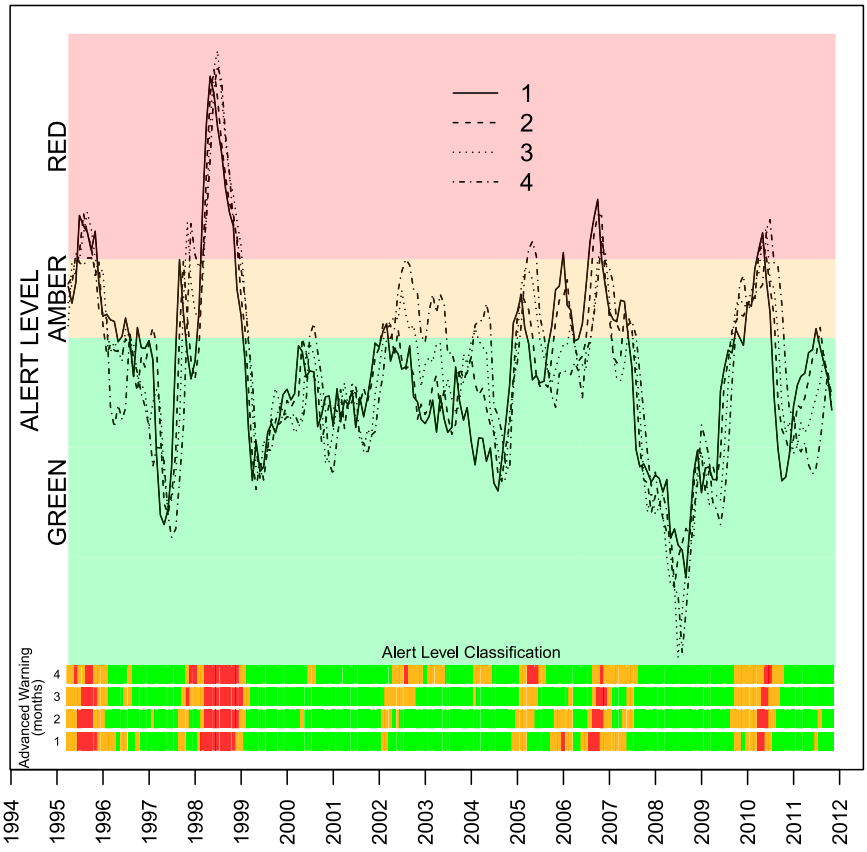

FIG. 5. Time series of ensemble-mean-normalized forecasts of the natural logarithm of the EIR averaged for altitudes exceeding 1500 m in the highlands of Uganda and Kenya with the annual cycle subtracted. Advance warnings (forecast lead time) of 1–4 months are shown. For example, the 4-month advance warning for June 2000 corresponds to a forecast that would be initialized at the beginning of March and issued shortly after, the issuing delay being due to the time necessary to run the forecast system and postprocess the results. A running mean is applied of 5 months to smooth the alert levels. For illustrative purposes the time series are nominally classified according to their mean percentile categories, with amber signifying an upper-tercile event and red indicating a 90th-percentile occurrence. The colored boxes below the plot indicate the indicative warning level that might be communicated to a decision maker at these four different advance-warning lead times.

limited to identifying the *potential* skill in such a system. Actual skill of the operational forecasts will be lower because of the use of an imperfect malaria model, and uncertainties in health data will also reduce the assessed skill. In another sense, the assessment also represents a lower threshold of potential skill, since improvements in the climate and malaria observations and modeling systems will increase skill. As examples, Dutra et al. (2013) recently introduced a bias correction for analysis rainfall that dramatically improved seasonal forecast skill of a standardized precipitation index that will be introduced to the system that is presented here. Physics improvements to the forecast system (e.g., Jung et al. 2010) and malaria model will also increase skill over time. For the current system, a preliminary analysis in the East African highlands indicated that the potential skill may translate into demonstrable skill at predicting real outbreaks.

The next phase is under way, in collaboration with two health ministries in Africa, in which a detailed evaluation of the system at the health-district level is conducted. Such endeavors are complicated by the relatively short and often incomplete records of malaria cases available in most countries. Although case-confirmation percentages have improved through uptake of rapid diagnostic test kits (Zhao et al. 2012), there remains the need for improved clinical datasets for the comprehensive evaluation of MEWS required for their uptake. This interactive process will likely highlight areas of the malaria-modeling system in need of further development.

There is also the need to consider the integration of forecast information into the current decision-making

process. Guidance is required on the forecast products that are most useful at district and national levels and also on how best to communicate forecast uncertainty to decision makers to effectively complement existing planning strategy. Despite the wide evidence cited earlier that climate information could increase advance warnings and the cost effectiveness of malaria interventions (Worrall et al. 2008), earlier demonstrations of MEWS that were based on climate monitoring have not been widely adopted in an operational environment to assist planning in African health ministries. To a large extent, health decisions concerning drug distribution and interventions are still based on long-term-mean malaria-prevalence maps (Omumbo et al. 2013). The possible reasons for this state of affairs are many and include the fact that health ministries often follow the strategy of increasing the efficiency of disease-monitoring systems so as to improve the reaction time to the onset of epidemics (DaSilva et al. 2004; Checchi et al. 2006). The operational paradigm of using climate or other information sources to predict outbreaks in advance is often unfamiliar. Moreover, using climate information to predict outbreaks implies the incorporation of uncertainty into the decision-making process and the risk of costs associated with a prediction failure (termed a forecast miss). The potential benefits of such information may be deemed to be outweighed by the perceived risk to the decision maker of implementing a superfluous and costly preemptive mitigation action on the basis of incorrect or inaccurate guidance.

The above considerations serve to emphasize that integrating climate-forecast information into the decision-making process will require extensive, country-level evaluation of system past performance, including cost–loss analysis of potential intervention actions taken on the basis of the information (Murphy 1977). To carry out such an analysis adequately, improvements in the representation of model uncertainty and increased ensembles sizes will be necessary, since the current system uses a single weather-forecast-ensemble system to drive a single malaria model. Additional climate-forecasting systems and malaria models should improve the representation of model uncertainty (Hagedorn et al. 2005).

A further consideration is that appropriate actions that are based on forecast information will also depend on a country's malaria-intervention phase (malaria control, progress toward elimination, or postelimination surveillance). While forecasts may have such use in guiding timely interventions in hyperendemic zones where earlier-than-usual malaria transmission is predicted, here the emphasis has been on epidemic regions. There, one can envisage forecast information aiding a wide range of district-level management decisions in countries still in the phase of malaria control, such as

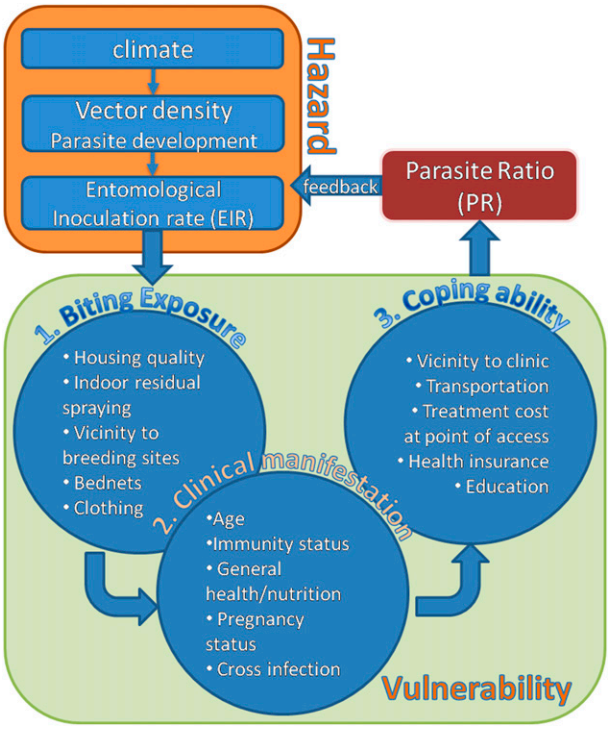

FIG. 6. Schematic of vulnerability considerations that could be considered as a three-tier process when combining with a climate-driven malaria-hazard forecast to determine local-scale population risk. The diagram emphasizes the coupled nature of the vector-borne disease. By lowering the local parasite burden, interventions that reduce a population's vulnerability also act to reduce subsequent climate-related hazard.

ensuring adequate drug supply to clinics and reassigning IRS teams to at-risk districts (Cox and Abeku 2007). District offices could also use forecast information to enhance information campaigns to vulnerable populations to increase bite-avoidance behaviors such as ensuring the use of nets supplied in previous mass-distribution campaigns, possibly through established local-level volunteer networks such as that of the International Federation of the Red Cross. This may involve combination of the malaria-hazard forecasts with high-spatial-resolution modeling of population vulnerability (Thomson and Connor 2001), which can change dramatically over small spatial scales (Carter et al. 2000). An example of a decision-support tool intended to serve such a purpose was recently presented by Kienberger and Hagenlocher (2014).

Consideration of societal vulnerability involves a plethora of different factors that require attention. One approach to consider these factors could be to divide the vulnerability factors into a three-tier sequential process as depicted in the schematic of Fig. 6, which is based on the framework of Kienberger and Hagenlocher (2014). Given a local transmission intensity as measured by the

EIR, the first "phase" would be to consider an individual's vulnerability to receiving an infectious bite, which entails their housing quality, their clothing choice, and their specific attractiveness to the mosquito vector (Burkot 1988; Lindsay et al. 1993; Knols et al. 1995). In the VECTRI dynamical malaria model this probability is considered to be equal for all members of society, but this is obviously an oversimplification. Furthermore, interventions such as IRS and the use of bednets are designed to greatly reduce an individual's exposure, the second element that contributes to overall risk.

In the final links of the risk chain, the vulnerability of an individual relates to the probability of an infective bite leading to a clinical manifestation of the disease. This is primarily determined by the individual's immune status, itself a function of previous exposure, in addition to age, presence of cross infection, nutrition, or the state of pregnancy (Doolan et al. 2009). Thereafter, one must consider the coping ability of the individual, connected to their potential to receive adequate and timing treatment in the case of a serious manifestation of the disease. These indicators are primarily economic or poverty related, essentially determining the overall cost to individuals to obtain treatment for themselves or their children. It is obvious that poverty ultimately determines many of the vulnerability factors in all three phases.

The schematic also underlines how both the transmission hazard and the societal vulnerability combine to determine the overall risk in a given location and thus the prevalence rate, which then affects future transmission hazard in a feedback because of the fully coupled nature of the system. This indicates that considering social vulnerability separately from hazard modeling in a so-called offline approach, as is often implemented in other fields, may not be adequate and that a fully integrated modeling system may be required to assess overall risk at the local level. A full consideration of the integration of climate information into health decision-making processes will be the natural next step.

Acknowledgments. This research was supported by the European Commission's Seventh Framework Research Programme under Quantifying Weather and Climate Impacts on Health in Developing Countries (QWeCI; Grant Agreement 243964) and HEALTHY FUTURES (266327). We thank S. Kienberger and M. Hagenlocher for advice on the issue of spatial modeling of vulnerability. The forecast data used for this paper were obtained from ECMWF's databases, and the authors do not have third-party dissemination rights. ECMWF should be contacted directly concerning data-access queries.

APPENDIX

Seamless Weather and Climate Prediction

Most operational forecasting centers run multiple forecasting systems to provide climate information at the relevant lead time for the varying sectors (e.g., hydrology, energy, health, or agriculture). A short-range high-resolution forecast usually provides deterministic predictions for several days ahead, whereas ensembles of lower-resolution, coupled models provide seasonal predictions up to 6 months or more in advance.

Some centers, such as ECMWF, bridge the gap between the two with an extended-range ensemble prediction system (Vitart et al. 2008). The system at ECMWF originally provided 51 forecasts for the next 32 days once per week each Thursday, which has recently been increased to a frequency of 2 times per week, and is referred to as the monthly system. Each 51-member "real time" forecast ensemble made in the present is matched with an additional set of forecast ensembles that start on the same day for each of the previous 18 years, referred to as hindcasts. For example, if a forecast (ensemble) is made starting on 1 June 2013, the system also runs an ensemble of hindcasts initialized on 1 June 1995, then 1 June 1996, and on to 2012. Because of the computational cost, the hindcast ensemble employs 5 members only, much fewer than the 51 members of the real-time forecast (and also somewhat less than the hindcast datasets available in the DEMETER and ENSEMBLES projects). This set of hindcasts allows the real-time predictions to be bias corrected and calibrated, since, although the ECMWF forecasting systems are considered to be state of the art in terms of their predictive skill (Hagedorn et al. 2012), they are nevertheless subject to systematic biases.

In the development of the seasonal-malaria-forecast system, rather than using only the seasonal-forecast system to drive the malaria model, it was decided to substitute this information with the monthly system for days 1–32 of the forecast. This is because the latter system is presumed to have superior forecast skill for climate parameters relative to the seasonal system for several reasons. The first is that the shorter forecast allows the monthly system to employ higher horizontal resolution, which, statistically for many forecasts, has been shown to improve ECMWF model skill (e.g., Jung et al. 2006, 2012; Magnusson and Källén 2013). In addition to the higher resolution, another reason to employ the monthly system is that, in common with the 10-day deterministic forecast, it takes advantage of regular updates and improvements to the physics parameterizations and analysis systems. These occur three

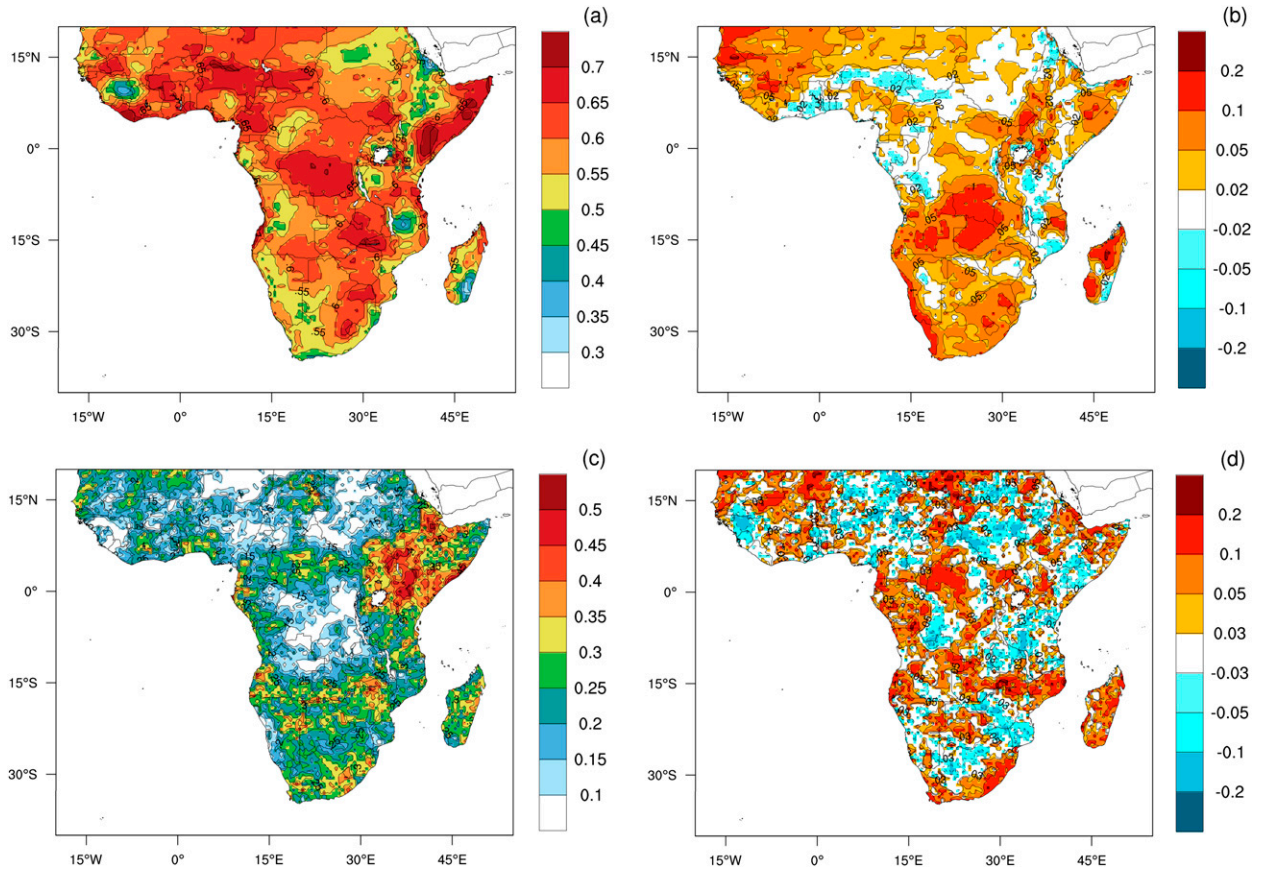

FIG. A1. Day 1–32, five-member ensemble-mean hindcast anomaly-correlation statistics averaged over the 12 start dates in 2012 (first Thursday in each month) for the 19-yr period 1994–2012: (a) temperature monthly system validated with ERA-Interim, (b) monthly system minus seasonal system 4, (c) precipitation monthly system validated with FEWS ARC2, and (d) monthly system minus seasonal system 4.

or four times per year, and this implies that the system is always fully state of the art (Jung et al. 2010). In contrast, the numerical cost of the hindcast suite prohibits this for the seasonal-forecast system, which is updated only every 3–5 years. Thus, depending on the date of the most recent seasonal-forecast-system update, the physics and associated climate biases can be considerably different between the two systems. Last of all, but potentially the most important, is that the more frequent issuing of the monthly forecasts gives them a considerable lead-time advantage. Using only the seasonal forecast system implies that forecast information can be updated at most once per month. Instead, use of the monthly system means that refreshed forecast information can be issued at least once per week. A forecast issued in the last week of the month has at least a 3-week lead-time advantage over the most recent seasonal forecast, for example. Note that for the forecast start dates chosen in this study (the first Thursday of each calendar month) this lead-time effect is limited to approximately 3 days.

To demonstrate the difference in skill for the monthly system relative to the seasonal system for days 1–32, we calculate the difference in anomaly correlation for temperature and precipitation for the 12 forecast dates used in this study. To do this, the exact 32 days from the seasonal forecast are extracted that match the monthly system. The rainfall is evaluated against FEWS ARC2 daily precipitation (Love 2002), and temperature is compared with ERA-Interim reanalysis data (Dee et al. 2011).

The temperature anomaly correlation lies in the range of 0.5–0.8 throughout most of Africa in the monthly system (Fig. A1a), which is statistically skillful. The increase in anomaly correlation gained by using the monthly system rather than the seasonal-forecast system is considerable (Fig. A1b), with a positive impact seen throughout much of the continent and the increase exceeding 10% in places. The rainfall skill is much lower, as expected, with correlations of zero in regions of the central Sahel and throughout the Congo. The latter may not be simply due to a poor forecast, since the lack of in

situ observations also leads to high uncertainties in retrieval products over this region (Washington et al. 2013). Correlations are higher over parts of southern Africa, and in particular for the Horn of Africa, approaching values of 0.5. This agrees with the conclusions drawn using ERA-Interim data in the main analysis of this paper. Note that statistical models also have success in predicting seasonal rainfall in this region (Mutai et al. 1998; Philippon et al. 2002; Hastenrath et al. 2004), although their output cannot be used to drive the dynamical disease models that require daily-time-scale input. For precipitation, the gain obtained by using the monthly system for the 12 start dates selected is less systematically positive than for temperature. Averaged for the region selected, the gain is a more modest value of approximately 0.02.

REFERENCES

Abeku, T. A., S. I. Hay, S. Ochola, P. Langi, B. Beard, S. J. de Vlas, and J. Cox, 2004: Malaria epidemic early warning and detection in African highlands. *Trends Parasitol.,* **20,** 400–405, doi:10.1016/j.pt.2004.07.005.

Alonso, D., M. J. Bouma, and M. Pascual, 2011: Epidemic malaria and warmer temperatures in recent decades in an East African highland. *Proc. Roy. Soc. London,* **278B,** 1661–1669, doi:10.1098/rspb.2010.2020.

Beier, J. C., J. Keating, J. I. Githure, M. B. Macdonald, D. E. Impoinvil, and R. J. Novak, 2008: Integrated vector management for malaria control. *Malar. J.,* **7** (Suppl. 1), doi:10.1186/1475-2875-7-S1-S4.

Bomblies, A., J. B. Duchemin, and E. A. B. Eltahir, 2009: A mechanistic approach for accurate simulation of village scale malaria transmission. *Malar. J.,* **8,** 223, doi:10.1186/1475-2875-8-223.

Bousema, T., and Coauthors, 2012: Hitting hotspots: Spatial targeting of malaria for control and elimination. *PLoS Med.,* **9,** e1001165, doi:10.1371/journal.pmed.1001165.

Burkot, T. R., 1988: Non-random host selection by anopheline mosquitoes. *Parasitol. Today,* **4,** 156–162, doi:10.1016/0169-4758(88)90151-2.

Caminade, C., and Coauthors, 2014: Impact of climate change on global malaria distribution. *Proc. Natl. Acad. Sci. USA,* **111,** 3286–3291, doi:10.1073/pnas.1302089111.

Carter, R., K. N. Mendis, and D. Roberts, 2000: Spatial targeting of interventions against malaria. *Bull. W. H. O.,* **78,** 1401–1411.

Ceccato, P., and Coauthors, 2007: Malaria stratification, climate, and epidemic early warning in Eritrea. *Amer. J. Trop. Med. Hyg.,* **77,** 61–68.

Checchi, F., J. Cox, S. Balkan, A. Tamrat, G. Priotto, K. P. Alberti, D. Zurovac, and J.-P. Guthmann, 2006: Malaria epidemics and interventions, Kenya, Burundi, southern Sudan, and Ethiopia, 1999–2004. *Emerg. Infect. Dis.,* **12,** 1477–1485, doi:10.3201/eid1210.060540.

Cox, J., and T. A. Abeku, 2007: Early warning systems for malaria in Africa: From blueprint to practice. *Trends Parasitol.,* **23,** 243–246, doi:10.1016/j.pt.2007.03.008.

——, S. I. Hay, T. A. Abeku, F. Checchi, and R. W. Snow, 2007: The uncertain burden of *Plasmodium falciparum* epidemics in Africa. *Trends Parasitol.,* **23,** 142–148, doi:10.1016/j.pt.2007.02.002.

Craig, M. H., R. W. Snow, and D. le Sueur, 1999: A climate-based distribution model of malaria transmission in sub-Saharan Africa. *Parasitol. Today,* **15,** 105–111, doi:10.1016/S0169-4758(99)01396-4.

DaSilva, J., B. Garanganga, V. Teveredzi, S. M. Marx, S. J. Mason, and S. J. Connor, 2004: Improving epidemic malaria planning, preparedness and response in southern Africa. *Malar. J.,* **3,** 37, doi:10.1186/1475-2875-3-37.

Dee, D. P., and Coauthors, 2011: The ERA-Interim reanalysis: Configuration and performance of the data assimilation system. *Quart. J. Roy. Meteor. Soc.,* **137,** 553–597, doi:10.1002/qj.828.

Di Giuseppe, F., F. Molteni, and E. Dutra, 2013a: Real-time correction of ERA-Interim monthly rainfall. *Geophys. Res. Lett.,* **40,** 3750–3755, doi:10.1002/grl.50670.

——, A. M. Tompkins, and F. Molteni, 2013b: A rainfall calibration methodology for impacts modelling based on spatial mapping. *Quart. J. Roy. Meteor. Soc.,* **139,** 1389–1401, doi:10.1002/qj.2019.

Diro, G. T., A. M. Tompkins, and X. Bi, 2012: Dynamical downscaling of ECMWF ensemble seasonal forecasts over East Africa with RegCM3. *J. Geophys. Res.,* **117,** D16103, doi:10.1029/2011JD016997.

Doolan, D. L., C. Dobano, and J. K. Baird, 2009: Acquired immunity to malaria. *Clin. Microbiol. Rev.,* **22,** 13–38, doi:10.1128/CMR.00025-08.

Dutra, E., F. Di Giuseppe, F. Wetterhall, and F. Pappenberger, 2013: Seasonal forecasts of droughts in African basins using the standardized precipitation index. *Hydrol. Earth Syst. Sci.,* **17,** 2359–2373, doi:10.5194/hess-17-2359-2013.

Feudale, L., and A. M. Tompkins, 2011: A simple bias correction technique for modeled monsoon precipitation applied to West Africa. *Geophys. Res. Lett.,* **38,** L03803, doi:10.1029/2010GL045909.

Gething, P. W., A. P. Patil, D. L. Smith, C. A. Guerra, I. R. F. Elyazar, G. L. Johnston, A. J. Tatem, and S. I. Hay, 2011: A new world malaria map: *Plasmodium falciparum* endemicity in 2010. *Malar. J.,* **10,** 378, doi:10.1186/1475-2875-10-378.

Gianotti, R. L., A. Bomblies, and E. A. B. Eltahir, 2009: Hydrologic modeling to screen potential environmental management methods for malaria vector control in Niger. *Water Resour. Res.,* **45,** W08438, doi:10.1029/2008WR007567.

Giorgi, F., R. Francisco, and J. Pal, 2003: Effects of a subgrid-scale topography and land use scheme on the simulation of surface climate and hydrology. Part I: Effects of temperature and water vapor disaggregation. *J. Hydrometeor.,* **4,** 317–333, doi:10.1175/1525-7541(2003)4<317:EOASTA>2.0.CO;2.

Githeko, A. K., and W. Ndegwa, 2001: Predicting malaria epidemics in the Kenyan highlands using climate data: A tool for decision makers. *Global Change Hum. Health,* **2,** 54–63, doi:10.1023/A:1011943131643.

Grover-Kopec, E., M. Kawano, R. W. Klaver, B. Blumenthal, P. Ceccato, and S. J. Connor, 2005: An online operational rainfall-monitoring resource for epidemic malaria early warning systems in Africa. *Malar. J.,* **4,** 6, doi:10.1186/1475-2875-4-6.

Hagedorn, R., F. J. Doblas-Reyes, and T. N. Palmer, 2005: The rationale behind the success of multi-model ensembles in seasonal forecasting—I. Basic concept. *Tellus,* **57A,** 219–233, doi:10.1111/j.1600-0870.2005.00103.x.

——, R. Buizza, T. M. Hamill, M. Leutbecher, and T. N. Palmer, 2012: Comparing TIGGE multimodel forecasts with reforecast-calibrated ECMWF ensemble forecasts. *Quart. J. Roy. Meteor. Soc.,* **138,** 1814–1827, doi:10.1002/qj.1895.

Hastenrath, S., D. Polzin, and P. Camberlin, 2004: Exploring the predictability of the 'short rains' at the coast of East Africa. *Int. J. Climatol.,* **24,** 1333–1343, doi:10.1002/joc.1070.

Hay, S. I., D. J. Rogers, G. D. Shanks, M. F. Myers, and R. W. Snow, 2001: Malaria early warning in Kenya. *Trends Parasitol.,* **17,** 95–99, doi:10.1016/S1471-4922(00)01763-3.

——, M. Renshaw, S. A. Ochola, A. M. Noor, and R. W. Snow, 2003a: Performance of forecasting, warning and detection of malaria epidemics in the highlands of western Kenya. *Trends Parasitol.,* **19,** 394–399, doi:10.1016/S1471-4922(03)00190-9.

——, E. C. Were, M. Renshaw, A. M. Noor, S. A. Ochola, I. Olusanmi, N. Alipui, and R. W. Snow, 2003b: Forecasting, warning, and detection of malaria epidemics: A case study. *J. Lancet,* **361,** 1705–1706, doi:10.1016/S0140-6736(03)13366-1.

——, C. A. Guerra, A. J. Tatem, A. M. Noor, and R. W. Snow, 2004: The global distribution and population at risk of malaria: Past, present, and future. *Lancet Infect. Dis.,* **4,** 327–336, doi:10.1016/S1473-3099(04)01043-6.

Hempel, S., K. Frieler, L. Warszawski, J. Schewe, and F. Piontek, 2013: A trend-preserving bias correction—The ISI-MIP approach. *Earth System Dyn.,* **4,** 219–236, doi:10.5194/esd-4-219-2013.

Hoshen, M. B., and A. P. Morse, 2004: A weather-driven model of malaria transmission. *Malar. J.,* **3,** 32, doi:10.1186/1475-2875-3-32.

Janowiak, J. E., V. E. Kousky, and R. J. Joyce, 2005: Diurnal cycle of precipitation determined from the CMORPH high spatial and temporal resolution global precipitation analyses. *J. Geophys. Res.,* **110,** D23105, doi:10.1029/2005JD006156.

Jones, A. E., and A. P. Morse, 2010: Application and validation of a seasonal ensemble prediction system using a dynamic malaria model. *J. Climate,* **23,** 4202–4215, doi:10.1175/2010JCLI3208.1.

——, and ——, 2012: Skill of ENSEMBLES seasonal re-forecasts for malaria prediction in West Africa. *Geophys. Res. Lett.,* **39,** L23707, doi:10.1029/2012GL054040.

——, U. U. Wort, A. P. Morse, I. M. Hastings, and A. S. Gagnon, 2007: Climate prediction of El Niño malaria epidemics in northwest Tanzania. *Malar. J.,* **6,** 162, doi:10.1186/1475-2875-6-162.

Jones, P. W., 1999: First- and second-order conservative remapping schemes for grids in spherical coordinates. *Mon. Wea. Rev.,* **127,** 2204–2210, doi:10.1175/1520-0493(1999)127<2204:FASOCR>2.0.CO;2.

Jung, T., S. K. Gulev, I. Rudeva, and V. Soloviov, 2006: Sensitivity of extratropical cyclone characteristics to horizontal resolution in the ECMWF model. *Quart. J. Roy. Meteor. Soc.,* **132,** 1839–1857, doi:10.1256/qj.05.212.

——, and Coauthors, 2010: The ECMWF Model Climate: Recent progress through improved physical parametrizations. *Quart. J. Roy. Meteor. Soc.,* **136,** 1145–1160, doi:10.1002/qj.634.

——, and Coauthors, 2012: High-resolution global climate simulations with the ECMWF model in Project Athena: Experimental design, model climate, and seasonal forecast skill. *J. Climate,* **25,** 3155–3172, doi:10.1175/JCLI-D-11-00265.1.

Kienberger, S., and M. Hagenlocher, 2014: Spatial-explicit modeling of social vulnerability to malaria in East Africa. *Int. J. Health Geogr.,* **13,** 29, doi:10.1186/1476-072X-13-29.

Kim, H.-M., P. J. Webster, and J. A. Curry, 2012: Seasonal prediction skill of ECMWF System 4 and NCEP CFSv2 retrospective forecast for the Northern Hemisphere winter. *Climate Dyn.,* **39,** 2957–2973, doi:10.1007/s00382-012-1364-6.

Kiszewski, A. E., and A. Teklehaimanot, 2004: A review of the clinical and epidemiologic burdens of epidemic malaria. *The Intolerable Burden of Malaria II: What's New, What's Needed,* J. Breman, M. S. Alilio, and A. Mills, Eds., Vol. 71.2, American Society of Tropical Medicine and Hygiene, 128–135.

Knols, B. G. J., R. de Jong, and W. Takken, 1995: Differential attractiveness of isolated humans to mosquitoes in Tanzania. *Trans. Roy. Soc. Trop. Med. Hyg.,* **89,** 604–606, doi:10.1016/0035-9203(95)90406-9.

Koram, K. A., S. Bennett, J. H. Adiamah, and B. M. Greenwood, 1995: Socio-economic risk factors for malaria in a peri-urban area of The Gambia. *Trans. Roy. Soc. Trop. Med. Hyg.,* **89,** 146–150, doi:10.1016/0035-9203(95)90471-9.

Kummerow, C., W. Barnes, T. Kozu, J. Shiue, and J. Simpson, 1998: The Tropical Rainfall Measuring Mission (TRMM) sensor package. *J. Atmos. Oceanic Technol.,* **15,** 809–817, doi:10.1175/1520-0426(1998)015<0809:TTRMMT>2.0.CO;2.

Li, Z.-L., B.-H. Tang, H. Wu, H. Ren, G. Yan, Z. Wan, I. F. Trigo, and J. A. Sobrino, 2013: Satellite-derived land surface temperature: Current status and perspectives. *Remote Sens. Environ.,* **131,** 14–37, doi:10.1016/j.rse.2012.12.008.

Linard, C., M. Gilbert, R. W. Snow, A. M. Noor, and A. J. Tatem, 2012: Population distribution, settlement patterns and accessibility across Africa in 2010. *PLoS ONE,* **7,** e31743, doi:10.1371/journal.pone.0031743.

Lindblade, K. A., E. D. Walker, A. W. Onapa, J. Katungu, and M. L. Wilson, 1999: Highland malaria in Uganda: Prospective analysis of an epidemic associated with El Niño. *Trans. Roy. Soc. Trop. Med. Hyg.,* **93,** 480–487, doi:10.1016/S0035-9203(99)90344-9.

Lindsay, S. W., J. H. Adiamah, J. E. Miller, R. J. Pleass, and J. R. M. Armstrong, 1993: Variation in attractiveness of human subjects to malaria mosquitoes (Diptera: Culicidae) in The Gambia. *J. Med. Entomol.,* **30,** 368–373.

Love, T., 2002: The Climate Prediction Center rainfall algorithm version 2. Climate Prediction Center Tech. Rep., 28 pp. [Available online at http://www.cpc.ncep.noaa.gov/products/fews/RFE2.ppt.]

Lowe, R., J. Chirombo, and A. M. Tompkins, 2013: Relative importance of climatic, geographic and socio-economic determinants of malaria in Malawi. *Malar. J.,* **12,** 416, doi:10.1186/1475-2875-12-416.

Lunde, T. M., M. N. Bayoh, and B. Lindtjørn, 2013: How malaria models relate temperature to malaria transmission. *Parasite Vectors,* **6,** 20, doi:10.1186/1756-3305-6-20.

Mabaso, M. L. H., and N. C. Ndlovu, 2012: Critical review of research literature on climate-driven malaria epidemics in sub-Saharan Africa. *Public Health,* **126,** 909–919, doi:10.1016/j.puhe.2012.07.005.

Magnusson, L., and E. Källén, 2013: Factors influencing skill improvements in the ECMWF forecasting system. *Mon. Wea. Rev.,* **141,** 3142–3153, doi:10.1175/MWR-D-12-00318.1.

Martens, P., and L. Hall, 2000: Malaria on the move: Human population movement and malaria transmission. *Emerg. Infect. Dis.,* **6,** 103–109, doi:10.3201/eid0602.000202.

Molteni, F., and Coauthors, 2011: The new ECMWF seasonal forecast system (System 4). ECMWF Tech. Rep. 656, 51 pp. [Available online at http://old.ecmwf.int/publications/library/ecpublications/_pdf/tm/601-700/tm656.pdf.]

Moonen, B., and Coauthors, 2010: Operational strategies to achieve and maintain malaria elimination. *Lancet,* **376,** 1592–1603, doi:10.1016/S0140-6736(10)61269-X.

Morse, A. P., F. J. Doblas-Reyes, M. B. Hoshen, R. Hagedorn, and T. N. Palmer, 2005: A forecast quality assessment of an end-to-end probabilistic multi-model seasonal forecast system using a malaria model. *Tellus,* **57A,** 464–475, doi:10.1111/j.1600-0870.2005.00124.x.

Murphy, A. H., 1977: The value of climatological, categorical and probabilistic forecasts in the cost-loss ratio situation. *Mon. Wea. Rev.,* **105,** 803–816, doi:10.1175/1520-0493(1977)105<0803:TVOCCA>2.0.CO;2.

——, and E. S. Epstein, 1989: Skill scores and correlation coefficients in model verification. *Mon. Wea. Rev.,* **117,** 572–582, doi:10.1175/1520-0493(1989)117<0572:SSACCI>2.0.CO;2.

Mutai, C., M. Ward, and A. Colman, 1998: Towards the prediction of the East Africa short rains based on sea surface temperature–atmosphere coupling. *Int. J. Climatol.,* **18,** 975–997, doi:10.1002/(SICI)1097-0088(199807)18:9<975::AID-JOC259>3.0.CO;2-U.

Nankabirwa, J., D. Zurovac, J. N. Njogu, J. B. Rwakimari, H. Counihan, R. W. Snow, and J. K. Tibenderana, 2009: Malaria misdiagnosis in Uganda—Implications for policy change. *Malar. J.,* **8,** 66, doi:10.1186/1475-2875-8-66.

Okiro, E. A., and R. W. Snow, 2010: The relationship between reported fever and *Plasmodium falciparum* infection in African children. *Malar. J.,* **9,** 99, doi:10.1186/1475-2875-9-99.

Omumbo, J. A., A. M. Noor, I. S. Fall, and R. W. Snow, 2013: How well are malaria maps used to design and finance malaria control in Africa? *PLoS ONE,* **8,** e53198, doi:10.1371/journal.pone.0053198.

Ototo, E. N., A. K. Githeko, C. L. Wanjala, and T. W. Scott, 2011: Surveillance of vector populations and malaria transmission during the 2009/10 El Niño event in the western Kenya highlands: Opportunities for early detection of malaria hyper-transmission. *Parasite Vectors,* **4,** 144, doi:10.1186/1756-3305-4-144.

Paaijmans, K. P., M. O. Wandago, A. K. Githeko, and W. Takken, 2007: Unexpected high losses of *Anopheles gambiae* larvae due to rainfall. *PLoS ONE,* **2,** e1146, doi:10.1371/journal.pone.0001146.

Palmer, T. N., and Coauthors, 2004: Development of a European Multimodel Ensemble System for Seasonal-to-Interannual Prediction (DEMETER). *Bull. Amer. Meteor. Soc.,* **85,** 853–872, doi:10.1175/BAMS-85-6-853.

Philippon, N., P. Camberlin, and N. Fauchereau, 2002: Empirical predictability study of October–December east African rainfall. *Quart. J. Roy. Meteor. Soc.,* **128,** 2239–2256, doi:10.1256/qj.01.190.

Piani, C., J. Haerter, and E. Coppola, 2009: Statistical bias correction for daily precipitation in regional climate models over Europe. *Theor. Appl. Climatol.,* **99,** 187–192, doi:10.1007/s00704-009-0134-9.

Piontek, F., and Coauthors, 2013: Multisectoral climate impact hotspots in a warming world. *Proc. Natl. Acad. Sci. USA,* **111,** 3233–3238, doi:10.1073/pnas.1222471110.

Roehrig, R., D. Bouniol, F. Guichard, F. Hourdin, and J.-L. Redelsperger, 2013: The present and future of the West African monsoon: A process-oriented assessment of CMIP5 simulations along the AMMA transect. *J. Climate,* **26,** 6471–6506, doi:10.1175/JCLI-D-12-00505.1.

Rogers, D. J., S. E. Randolph, R. W. Snow, and S. I. Hay, 2002: Satellite imagery in the study and forecast of malaria. *Nature,* **415,** 710–715, doi:10.1038/415710a.

Ropelewski, C. F., and M. S. Halpert, 1987: Global and regional scale precipitation patterns associated with El Niño/Southern Oscillation. *Mon. Wea. Rev.,* **115,** 1606–1626, doi:10.1175/1520-0493(1987)115<1606:GARSPP>2.0.CO;2.

Simmons, A. J., and A. Hollingsworth, 2002: Some aspects of the improvement in skill of numerical weather prediction. *Quart. J. Roy. Meteor. Soc.,* **128,** 647–677, doi:10.1256/003590002321042135.

Smith, D. L., J. Dushoff, R. W. Snow, and S. I. Hay, 2005: The entomological inoculation rate and *Plasmodium falciparum* infection in African children. *Nature,* **438,** 492–495, doi:10.1038/nature04024.

Smith, T., J. D. Charlwood, A. Y. Kitua, H. Masanja, S. Mwankusye, P. L. Alonso, and M. Tanner, 1998: Relationships of malaria morbidity with exposure to *Plasmodium falciparum* in young children in a highly endemic area. *Amer. J. Trop. Med. Hyg.,* **59,** 252–257.

Snow, R. W., M. Craig, U. Deichmann, and K. Marsh, 1999: Estimating mortality, morbidity and disability due to malaria among Africa's non-pregnant population. *Bull. W. H. O.,* **77,** 624–640.

Sultan, B., S. Janicot, and A. Diedhiou, 2003: The West African monsoon dynamics. Part I: Documentation of intraseasonal variability. *J. Climate,* **16,** 3389–3406, doi:10.1175/1520-0442(2003)016<3389:TWAMDP>2.0.CO;2.

Teklehaimanot, H. D., M. Lipsitch, A. Teklehaimanot, and J. Schwartz, 2004: Weather-based prediction of *Plasmodium falciparum* malaria in epidemic-prone regions of Ethiopia I. Patterns of lagged weather effects reflect biological mechanisms. *Malar. J.,* **3,** 41, doi:10.1186/1475-2875-3-41.

Thiemig, V., R. Rojas, M. Zambrano-Bigiarini, V. Levizzani, and A. De Roo, 2012: Validation of satellite-based precipitation products over sparsely gauged African river basins. *J. Hydrometeor.,* **13,** 1760–1783, doi:10.1175/JHM-D-12-032.1.

Thomson, M. C., and S. J. Connor, 2001: The development of malaria early warning systems for Africa. *Trends Parasitol.,* **17,** 438–445, doi:10.1016/S1471-4922(01)02077-3.

——, ——, N. Ward, and D. Molyneux, 2004: Impact of climate variability on infectious disease in West Africa. *EcoHealth,* **1,** 138–150, doi:10.1007/s10393-004-0004-y.

——, S. J. Mason, T. Phindela, and S. J. Connor, 2005: Use of rainfall and sea surface temperature monitoring for malaria early warning in Botswana. *Amer. J. Trop. Med. Hyg.,* **73,** 214–221. [Available online at http://www.ajtmh.org/content/73/1/214.full.pdf+html.]

——, F. J. Doblas-Reyes, S. J. Mason, R. Hagedorn, S. J. Connor, T. Phindela, A. P. Morse, and T. N. Palmer, 2006: Malaria early warnings based on seasonal climate forecasts from multi-model ensembles. *Nature,* **439,** 576–579, doi:10.1038/nature04503.

——, S. J. Connor, S. E. Zebiak, M. Jancloes, and A. Mihretie, 2011: Africa needs climate data to fight disease. *Nature,* **471,** 440–442, doi:10.1038/471440a.

Tompkins, A. M., and L. Feudale, 2010: West Africa monsoon seasonal precipitation forecasts in ECMWF System 3 with a focus on the AMMA SOP. *Wea. Forecasting,* **25,** 768–788, doi:10.1175/2009WAF2222236.1.

——, and V. Ermert, 2013: A regional-scale, high resolution dynamical malaria model that accounts for population density, climate and surface hydrology. *Malar. J.,* **12,** 65, doi:10.1186/1475-2875-12-65.

Vellinga, M., A. Arribas, and R. Graham, 2012: Seasonal forecasts for regional onset of the West African monsoon. *Climate Dyn.,* **40,** 3047–3070, doi:10.1007/s00382-012-1520-z.

Vitart, F., and Coauthors, 2008: The new VarEPS-monthly forecasting system: A first step towards seamless prediction. *Quart. J. Roy. Meteor. Soc.,* **134,** 1789–1799, doi:10.1002/qj.322.

Washington, R., R. James, H. Pearce, W. M. Pokam, and W. Moufouma-Okia, 2013: Congo basin rainfall climatology: Can we believe the climate models? *Philos. Trans. Roy. Soc. London,* **368B,** 20120296, doi:10.1098/rstb.2012.0296.

Weisheimer, A., and Coauthors, 2009: ENSEMBLES: A new multi-model ensemble for seasonal-to-annual predictions—Skill and progress beyond DEMETER in forecasting tropical

Pacific SSTs. *Geophys. Res. Lett.,* **36,** L21711, doi:10.1029/2009GL040896.

Worrall, E., A. Rietveld, and C. Delacollette, 2004: The burden of malaria epidemics and cost-effectiveness of interventions in epidemic situations in Africa. *The Intolerable Burden of Malaria II: What's New, What's Needed,* J. G. Breman, M. S. Alilio, and A. Mills, Eds., Vol. 71.2, American Society of Tropical Medicine and Hygiene, 136–140.

——, S. Connor, and M. C. Thomson, 2008: Improving the cost-effectiveness of IRS with climate informed health surveillance systems. *Malar. J.,* **7,** 263, doi:10.1186/1475-2875-7-263.

Yeka, A., and Coauthors, 2012: Malaria in Uganda: Challenges to control on the long road to elimination: I. Epidemiology and current control efforts. *Acta Trop.,* **121,** 184–195, doi:10.1016/j.actatropica.2011.03.004.

Yukich, J. O., and Coauthors, 2008: Costs and consequences of large-scale vector control for malaria. *Malar. J.,* **7,** 258, doi:10.1186/1475-2875-7-258.

Zhao, J., M. Lama, E. Korenromp, P. Aylward, E. Shargie, S. Filler, R. Komatsu, and R. Atun, 2012: Adoption of rapid diagnostic tests for the diagnosis of malaria, a preliminary analysis of the global fund program data, 2005 to 2010. *PLoS ONE,* **7,** e43549, doi:10.1371/journal.pone.0043549.